Speckle Suppression of OKG Imaging in Highly Turbid Medium Using SC-Assisted Fundamental Frequency

Yuhu Ren, Jinhai Si, Wenjiang Tan, Yipeng Zheng, Junyi Tong, and Xun Hou

***Abstract*— We propose a method to suppress the speckle of optical Kerr gated (OKG) imaging in highly turbid medium using an 800-nm femtosecond laser, in which, the 800-nm fundamental frequency light and the supercontinuum (SC) containing the fundamental frequency are used as the gating beam and imaging beam, respectively. A sequence of images of a test chart hidden behind a highly turbid medium is obtained using the OKG technique. Compared with images obtained with OKG imaging using only the fundamental frequency, the image resolution and contrast of images obtained through OKG imaging using the SC-assisted fundamental frequency are both significantly enhanced.**

***Index Terms*— Speckle, optical Kerr effect, turbid media, ultrafast optics.**

I. Introduction

LASER imaging of hidden objects in highly scattering media is important in many areas such as in the atmosphere, underwater, or in aerated sprays [1]. Many different techniques have been explored to detect objects embedded in turbid media [2]–[6]. However, the coherence of lasers leads to coherent imaging artifacts, which arise from the interference during image formation [7]. The most common manifestation of coherent artifacts is speckle [8]. Image quality is often degraded by speckle noise, which presents one of the challenges associated with laser imaging in scattering medium. Due to the different propagation times through turbid media between the scattered photons and the ballistic photons, a feasible way to suppress multiple scattered photons and improve the visualization of objects hidden in turbid media is using a time-gated technique. Several nonlinear optical effects, such as degenerate optical parametric amplification [9], second harmonic generation [10], and the optical Kerr effect have been used to realize the ultrafast time gate. Among the available time-gated imaging techniques, optical Kerr gated (OKG) imaging based on the optical Kerr effect has been widely used owing to its advantages, e.g., the phase-matching condition does not need to be satisfied. Furthermore, femtosecond OKG imaging provides an effective approach to obtaining single-shot images of high-speed mobile objects such as the structures in the high pressure spray region, which rapidly change on the time scale of a few microseconds [11]. In our experiment, when OKG is used for imaging in a highly turbid medium, the number of ballistic photons is insufficient to form an image. In this case, the snake photons that retain slightly distorted information need to be gated for imaging, although the snake photons lead to speckles which will result in the decrease of the image quality. Therefore, it is necessary to suppress speckle of OKG imaging in highly turbid medium.

Over the years, various methods have been introduced to suppress the speckle in laser images in turbid media. The speckle in laser imaging can be suppressed by averaging the multiple images obtained using diverse wavelengths, or diverse polarizations, or by changing the illumination angle of the object [12]. A source containing a partially coherent light, such as a light-emitting diode (LED) was also applied to reduce the speckle noise [13]. This method cannot be used to suppress speckle in single-shot femtosecond OKG imaging in a spray. The speckle suppression approach is put forward by the digital processing methods, which have been widely applied to suppress the speckle in laser imaging [14]. However, these digital processing methods cause inevitable loss of object information and the speckle noise suppressions are limited [15]. Other techniques using incoherent, ultra-short pulsed illumination for time-gated ballistic imaging in turbid media have also been applied to suppress speckle noise [16]. In this method, the speckle of OKG imaging is suppressed by reducing the coherence of the imaging beam. This OKG imaging using the supercontinuum (SC) is mainly appropriate for imaging in moderately turbid medium since the power of the SC selected by the OKG is low.

In this letter, we propose an improved method to suppress the speckle of OKG imaging, which is appropriate for imaging

Manuscript received October 12, 2016; revised November 13, 2016; accepted November 14, 2016. Date of publication November 16, 2016; date of current version December 20, 2016. This work was supported in part by the National Natural Science Foundation of China under Grant 61235003, Grant 61427816, Grant 61205129, and Grant 61308036, in part by the Natural Science Basic Research Plan in Shaanxi Province of China under Grant 2014JQ8363, in part by the Open Found of State Key Laboratory on Integrated Optoelectronics under Grant IOSKL2015KF24, and in part by the Collaborative Innovation Center of Suzhou Nano Science and Technology. *(Corresponding author: Jinhai Si.)*

Y. Ren, J. Si, W. Tan, Y. Zheng, and X. Hou are with the Key Laboratory for Physical Electronics and Devices of the Ministry of Education & Shaanxi and the Key Laboratory of Information Photonic Technique, School of Electronics & Information Engineering, Xi'an Jiaotong University, Xi'an 710049, China (e-mail: jinhaisi@mail.xjtu.edu.cn).

J. Tong is with the Departments of Applied Physics, Xi'an University of Technology, Xi'an 710048, China.

Color versions of one or more of the figures in this letter are available online at http://ieeexplore.ieee.org.

Digital Object Identifier 10.1109/LPT.2016.2629498

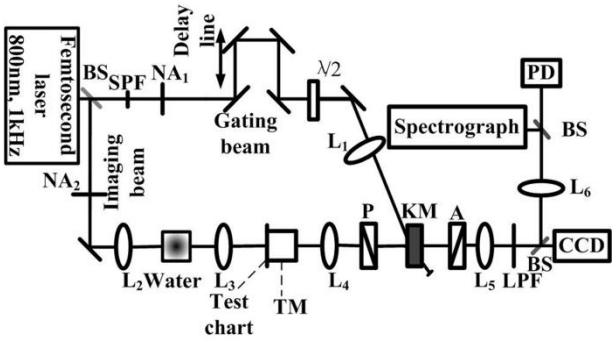

Fig. 1. Experimental setup for the OKG imaging system. L: lens; BS: beam splitter; SPF: short pass filter; $\lambda/2$: half-wave plate; P: polarizer; A: analyzer; NA: neutral attenuator; LPF: long pass filter; TM: turbid medium; KM: Kerr medium; BS: beam splitter.

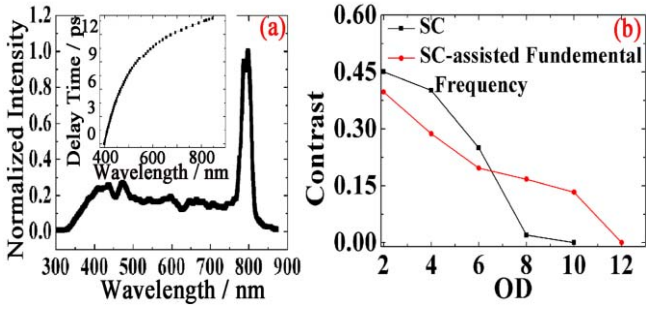

Fig. 2. (a) Whole ranges of the spectrum of the SC. The inset shows the chirp characteristics of the SC, (b) variation of contrast as a function of OD for the bars in Group 2 Element 6 of the test chart for OKG imaging using SC and SC-assisted fundamental frequency.

in highly turbid medium. The 800 nm fundamental frequency light and the SC containing the fundamental frequency with a wavelength from 780-870 nm are used as the gating beam and imaging beam respectively. A sequence of images of a test chart hidden behind a highly turbid medium is obtained using the OKG technique. Compared with images obtained with OKG imaging using only the fundamental frequency, the image resolution of those obtained with OKG imaging using the SC-assisted fundamental frequency is higher and the contrast is significantly enhanced.

II. Experimental Setup

The schematic of the OKG imaging system is shown in Fig. 1. A Ti: sapphire laser produced 800 nm, 50 fs pulses at a repetition rate of 1 kHz with a full width half maximum bandwidth of 40 nm. The laser beam was split into a gating beam centered at 790 nm and an imaging beam centered at 800 nm by a beam splitter (BS) and a short pass filter (SPF). The intensities of the gating and imaging beams were adjusted by neutral attenuators (NA_1 and NA_2). The imaging beam was first focused by lens L_2 with a focal length of 150 mm into a 5-cm-long water cell to generate a SC. The SC was collimated by lens L_3 with a focal length of 100 mm. The imaging beam was modulated by a U.S. Air Force resolution chart with 1.41-line-pair/mm and then introduced to a turbid medium. The transmitted light from the turbid medium was first focused by lens L_4 and then introduced into the OKG. The gating beam was first linearly polarized at 45° with respect to the polarization of the imaging beam for optimal efficiency using a half-wave ($\lambda/2$) plate. Thereafter, the gating beam was focused into the Kerr medium of a 5-mm CS_2 filled quartz cell. A long pass filter (LPF) was placed before the BS to block light noise caused by the gating beam scattered forward into the detecting devices. In this setup, the imaging pulse was spatially overlapped with the gating pulse in the Kerr medium, which was placed at the focal plane of lens L_4. The lens L_5 is used to adjust the magnification of the imaging system. When the two pulses were spatially and temporally overlapped, the imaging pulse polarization was rotated due to the birefringence of the Kerr medium induced by the gating pulse [17]. Part of the imaging pulse was then passed through the analyzer, which was synchronously detected by a charge coupled device (CCD) camera, a photodiode (PD), and a spectrograph (Ocean Optics USB2000).

The turbid medium was composed of a silica microsphere solution contained in a cubic cuvette. The thickness of the cuvette along the optical axis was 10 mm. The diameter of the silica microspheres was 5.65 μm. The optical depth (OD) of the sample was changed by dilution. In our experiment, the turbid medium is located after the test chart for better demonstrating the role of the OKG. The image contrast increases with the test chart embedded in the scattering sample without OKG, which will decrease the necessity of using the OKG [18]. Although OKG imaging is used for transillumination imaging in this experiment, it is also valid for time-gated backscatter imaging [19].

III. Results and Discussion

In our experiment, the LPF is removed from the experimental setup when we measure the chirp characteristics of the SC. The whole range of the spectrum of the SC is shown in Fig. 2(a). The SC shows a positive chirp, as shown in the inset of Fig. 2(a). The spectrum width selected by the OKG increases with an increase in delay time, which arises from the chirp characteristics of the SC and the certain switching time of OKG of CS_2. Furthermore, we compare intensity of the imaging beam selected by the OKG using the SC-assisted fundamental frequency with that using only part of the SC. In our experiment, the gating efficiency of the OKG is about 0.45. The intensity of the imaging beam selected by the OKG can be calculated using $I = 0.45 \int_{\lambda 1}^{\lambda 2} I(\lambda) d\lambda$.When OKG imaging uses the SC-assisted fundamental frequency (780-870 nm), the intensity of the imaging beam selected by the OKG is 12.5. When OKG imaging only use part of SC (560 – 635 nm), the intensity of the imaging beam selected by the OKG is 5.5. The imaging pulse intensity of OKG imaging using the SC-assisted fundamental frequency is higher than OKG imaging using only part of SC. Further, the variation of image contrast as a function of OD for the bars in Group 2 Element 6 of the test chart is shown in Fig.2 (b). As shown in Fig. 2(b), the OKG imaging using SC can be used for imaging in moderately turbid medium (OD $<$ 8). The OKG imaging using

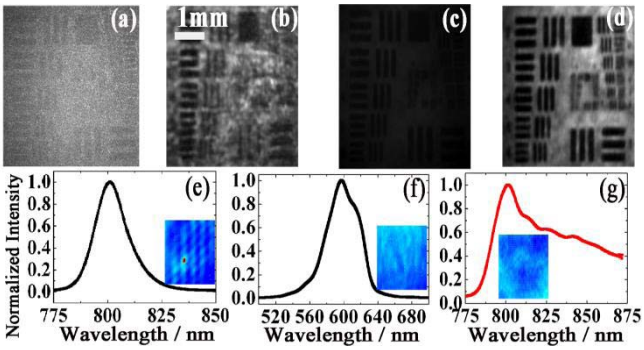

Fig. 3. Images of the test chart behind the silica microsphere sample and the corresponding spectrum selected by the OKG. (a) No time gate (standard transillumination), (b) OKG imaging using fundamental frequency, (c) OKG imaging using part of SC, (d) OKG imaging using SC-assisted fundamental frequency, (e) spectrum of the fundamental frequency, the inset shows the interference pattern (f) spectrum of part of the SC, the inset shows the interference pattern (g) spectrum of the SC-assisted fundamental frequency, the inset shows the interference pattern.

SC-assisted fundamental frequency can be used for imaging in highly turbid medium (OD > 9) [20]. In moderately turbid medium, the image contrasts by using SC are higher than those by using SC-assisted fundamental frequency, which arises from the different speckle suppression. The speckle in the OKG imaging using SC is minor because the coherence of the SC pulse is lower than that of the SC-assisted fundamental frequency pulse. In highly turbid medium, the imaging pulse intensity of OKG imaging using part of SC is not enough for imaging, which decreases the image contrast. The contrast is defined as $C(f) = (I_{\max} - I_{\min}) / (I_{\max} + I_{\min})$ [21], where f is the spatial frequency.

Furthermore, we compare the result of speckle suppression of our method with that of the OKG imaging using part of the SC. The images of a test chart hidden behind a silica microsphere sample (OD = 8.0) are demonstrated using the OKG technique. In Fig. 3(a), we show direct imaging for the sample filled with the silica microsphere turbid medium. In Fig. 3(b), we show OKG imaging using only the fundamental frequency. In Figs. 3(c) and 3(d), we show OKG imaging using part of the SC and the SC-assisted fundamental frequency, respectively. In Figs. 3(e), 3(f), and 3(g), we show the normalized spectrum of the fundamental frequency, part of the SC, and the SC-assisted fundamental frequency, respectively. In Fig. 3 (a), the object hidden behind such a turbid medium cannot be seen because the total intensity of the scattered photons is greater than the intensity of the ballistic photons. As shown in Fig. 3(b), the image resolution decreases although the contrast of the image is improved. The decreased image resolution resulting from OKG imaging using only the fundamental frequency can be attributed to the speckle noise in the image, which arises from the coherence of the residual scattered photons. In Fig. 3(c), the image cannot be seen clearly. From Fig. 3 (d), we can see that most of the speckle noise of the OKG image is removed and the visibility of image is enhanced. It should be noted that the spectrum of the imaging beam selected from the SC is restricted by the gating beam to decrease the coherence effect in the Kerr medium. In this experiment, although the spectrum of the SC-assisted fundamental frequency slightly overlaps with that of the gating beam, the coherence effect in the Kerr medium is not serious due to the different central wavelengths and different polarized directions of the two beams.

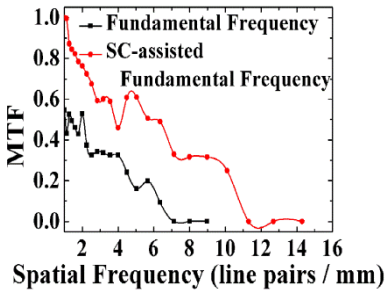

Fig. 4. Comparison of the MTF of OKG imaging using the fundamental frequency system and OKG imaging using the SC-assisted fundamental frequency system.

The difference between OKG imaging using only the fundamental frequency and the SC-assisted fundamental frequency can be explained as follows. The speckle pattern on the image plane is the incoherent combination of the intensity of different wavelengths. The superposition of the speckle pattern of different wavelengths results in the reduction of speckle contrast since the speckle patterns are different for light with different wavelengths. The ratio of speckle contrast before and after the spectrum expansion is $C_s/C_{s0} = 1\Big/\sqrt{1+(2W\sigma)^2}$, where C_{s0} and C_s are the speckle contrast before and after the spectrum expansion respectively, W is the width of spectrum and σ is the standard deviation of the optical path fluctuations [22]. From Figs. 3(e) and 3(g), we can see that the spectrum range of the fundamental frequency and the SC-assisted fundamental frequency are 780-820 nm and 780-870 nm, respectively. Furthermore, in the same turbid medium sample, the standard deviation of the optical path fluctuations did not change. The contrast of the speckle decreased with an increase of in spectrum width. Further, the temporal coherence of the fundamental frequency, SC, and SC-assisted fundamental frequency pulses were estimated using a Mach–Zehnder interferometer setup. The interference pattern for the fundamental frequency pulses can be seen clearly. The coherence of the SC-assisted fundamental frequency pulses decrease compared with the fundamental frequency pulses as show in the insets of Figs.3(e) and 3(g). Hence, the speckle contrast of images obtained using OKG imaging with the SC-assisted fundamental frequency decreased.

To further quantitatively evaluate the performance of the two OKG imaging systems, we measured the modulation transfer function (MTF) of both systems. The MTF is given by $MTF(f) = C(f)/C_0(f)$, where $C_0(f)$ denotes the modulation of the object. From Fig. 4, we see that the spatial resolution of OKG imaging using the SC-assisted fundamental frequency system is higher than that of OKG imaging using only the fundamental frequency system. For OKG imaging using the fundamental frequency system, the maximum resolvable spatial frequency is 7.13 line pairs per millimeter (lp/mm), with a resolved object size of approximately 70.15 μm.

However, for OKG imaging using the SC-assisted fundamental frequency system, the maximum resolvable spatial frequency is 11.3 lp/mm, with a resolved object size of approximately 44.19 μm. The results show that OKG imaging using the SC-assisted fundamental frequency could suppress the speckle, thus, providing a higher resolvable spatial frequency and a higher contrast.

IV. Conclusions

In conclusion, a method to suppress the speckle of OKG imaging in highly turbid media is demonstrated, in which, the 800 nm fundamental frequency light and the SC containing the fundamental frequency are used as the gating beam and imaging beam, respectively. A sequence of images of a test chart hidden behind a highly scattering medium was obtained using the OKG. The contrast of images obtained with OKG imaging using the SC-assisted fundamental frequency is significantly enhanced.

References

[1] D. Sedarsky, J. Gord, C. Carter, T. Meyer, and M. Linne, "Fast-framing ballistic imaging of velocity in an aerated spray," *Opt. Lett.*, vol. 34, no. 18, pp. 2748–2750, 2009.

[2] H. L. Xu and S. L. Chin, "Femtosecond laser filamentation for atmospheric sensing," *Sensors*, vol. 11, no. 1, pp. 32–53, 2011.

[3] B. J. Vakoc, D. Fukumura, R. K. Jain, and B. E. W. Bouma, "Cancer imaging by optical coherence tomography: Preclinical progress and clinical potential," *Nature Rev. Cancer*, vol. 12, pp. 363–368, 2012.

[4] A. P. Mosk, A. Lagendijk, G. Lerosey, and M. Fink, "Controlling waves in space and time for imaging and focusing in complex media," *Nature Photon.*, vol. 6, pp. 283–292, May 2012.

[5] S. M. Popoff, G. Lerosey, R. Carminati, M. Fink, A. C. Boccara, and S. Gigan, "Measuring the transmission matrix in optics: An approach to the study and control of light propagation in disordered media," *Proc. PRL*, vol. 104, pp. 100601–100604, Mar. 2010.

[6] Z. Yaqoob, D. Psaltis, M. S. Feld, and C. Yang, "Optical phase conjugation for turbidity suppression in biological samples," *Nature Photon.*, vol. 2, pp. 110–115, Jan. 2008.

[7] D. Kim, "Reduction of coherent artifacts in dynamic holographic three-dimensional displays by diffraction-specific pseudorandom diffusion," *Opt. Lett.*, vol. 29, no. 6, pp. 611–613, 2004.

[8] B. Redding, M. A. Choma, and H. Cao, "Speckle-free laser imaging using random laser illumination," *Nature Photontics*, vol. 6, pp. 355–359, Apr. 2012.

[9] J. Watson, P. Georges, T. Lépine, B. Alonzi, and A. Brun, "Imaging in diffuse media with ultrafast degenerate optical parametric amplification," *Opt. Lett.*, vol. 20, no. 3, pp. 231–233, 1995.

[10] R. Ambekar, T.-Y. Lau, M. Walsh, R. Bhargava, and K. C. Toussaint, Jr., "Quantifying collagen structure in breast biopsies using second-harmonic generation imaging," *Biomed. Opt. Exp.*, vol. 3, no. 9, pp. 2021–2035, 2012.

[11] M. Paciaroni and M. Linne, "Single-shot, two-dimensional ballistic imaging through scattering media," *Appl. Opt.*, vol. 43, no. 26, pp. 5100–5109, 2004.

[12] J. G. Manni and J. W. Goodman, "Versatile method for achieving 1% speckle contrast in large-venue laser projection displays using a stationary multimode optical fiber," *Opt. Exp.*, vol. 20, no. 10, pp. 11288–11315, 2012.

[13] C. Remmersmann, S. Stürwald, B. Kemper, P. Langehanenberg, and G. Bally, "Phase noise optimization in temporal phase-shifting digital holography with partial coherence light sources and its application in quantitative cell imaging," *Appl. Opt.*, vol. 48, no. 8, pp. 1463–1472, 2009.

[14] V. Bianco, M. Paturzo, P. Memmolo, A. Finizio, P. Ferraro, and B. Javidi, "Random resampling masks: A non-Bayesian one-shot strategy for noise reduction in digital holography," *Opt. Lett.*, vol. 38, no. 5, pp. 619–621, 2013.

[15] J. Leng, J. Zhou, X. Lang, and X. Li, "Two-stage method to suppress speckle noise in digital holography," *Opt. Rev.*, vol. 22, no. 5, 844-852, 2015.

[16] H. Purwar, S. Idlahcen, C. Rozé, and J. B. Blaisot. (2015). "Time-resolved imaging with OKE-based time-gate: Enhancement in spatial resolution using low-coherence ultra-short illumination." [Online]. Available: https://arxiv.org/abs/1502.07255

[17] F. Mathieu, M. A. Reddemann, J. Palmer, and R. Kneer, "Time-gated ballistic imaging using a large aperture switching beam," *Opt. Exp.*, vol. 22, no. 6, pp. 7058–7074, 2014.

[18] L. Wang, P. Ho, X. Liang, H. Dai, and R. Alfano, "Kerr–Fourier imaging of hidden objects in thick turbid media," *Opt. Lett.*, vol. 18, no. 3, pp. 241–243, 1993.

[19] M. Rahm, Z. Falgout, D. Sedarsky, and M. Linne, "Optical sectioning for measurements in transient sprays," *Opt. Exp.*, vol. 24, no. 5, pp. 4610–4621, 2016.

[20] E. Berrocal, D. Sedarsky, M. Paciaroni, I. Meglinski, and M. Linne, "Laser light scattering in turbid media part I: Experimental and simulated results for the spatial intensity distribution," *Opt. Exp.*, vol. 15, no. 17, pp. 10649–10665, 2007.

[21] Y. Ren, J. Si, W. Tan, S. Xu, J. Tong, and X. Hou, "Microscopic imaging through a turbid medium by use of a differential optical Kerr gate," *IEEE Photon. Technol. Lett.*, vol. 28, no. 4, pp. 394–397, Apr. 15, 2016.

[22] Z. Cui *et al.*, "Speckle suppression by controlling the coherence in laser based projection systems," *J. Display Technol.*, vol. 11, no. 4, pp. 330–335, Apr. 2015.